



Published in final edited form as:

Chemistry. 2005 February 4; 11(4): 1137–1144.

## Modulating Charge Transfer Through Cyclic D,L $\alpha$ -Peptide Self-Assembly

W. Seth Horne<sup>[a]</sup>, Nurit Ashkenasy<sup>[a]</sup>, and M. Reza Ghadiri<sup>\*</sup>

Departments of Chemistry and Molecular Biology and The Skaggs, Institute for Chemical Biology, The Scripps Research Institute, 10550 North Torrey Pines Rd., La Jolla, California 92037 (USA)

### Abstract

We describe a concise solid support-based synthetic method for the preparation of cyclic D,L  $\alpha$ -peptides bearing 1,4,5,8-naphthalenetetracarboxylic diimide (NDI) side chains. Studies of the structural and photoluminescence properties of these molecules in solution show that the hydrogen bond directed self-assembly of the cyclic D,L  $\alpha$ -peptide backbone promotes intermolecular NDI excimer formation. The efficiency of NDI charge transfer in the resulting supramolecular assemblies is shown to depend on the length of the linker between the NDI and the peptide backbone, the distal NDI substituent, and the number of NDIs incorporated in a given structure. The design rationale and synthetic strategies described here should provide a basic blueprint for a series of self-assembling cyclic D,L  $\alpha$ -peptide nanotubes with interesting optical and electronic properties.

### Keywords

charge transfer; cyclic peptides; self-assembly; supramolecular chemistry; nanotubes

### Introduction

Cyclic D,L  $\alpha$ -peptides are the archetypical member of a growing class of organic tubular supramolecular structures<sup>[1–8]</sup> with promising applications in biological<sup>[9]</sup> and materials<sup>[10]</sup> settings. Due to increasing interest in the field of molecular electronics<sup>[11]</sup>, theoretical calculations have been used to assess the conductive properties of self-assembling peptide nanotubes.<sup>[12]</sup> It has been proposed that the cyclic D,L  $\alpha$ -peptide structures possess a wide band gap ( $E_g > 4$  eV) that could potentially be tuned by appropriate modifications to the cyclic peptide.<sup>[12d]</sup> However, it has been determined that natural amino acid side chains cannot be used to decrease the band gap to levels sufficient for potential use in molecular electronics applications. Considering that many organic semiconducting and conducting materials are based on one dimensional stacking of aromatic molecules through  $\pi$ - $\pi$  interactions and partial charge transfer<sup>[13]</sup>, we envisioned that cyclic peptide self-assembly might be useful in controlling and directing the stacking of aromatic side chains and offer a level of control over the long range order in the resulting materials.<sup>[1, 10b, 14]</sup>

Among aromatic molecules that have found utility in the design of conductive materials, naphthalenediimide (NDI) derivatives have drawn considerable attention due to their tendency to form n-type materials, as opposed to most other organic molecules used to fabricate p-type semiconductors.<sup>[15]</sup> High conductivity materials based on NDI derivatized dendrimers and polymers have also been reported.<sup>[16]</sup> We postulated that the intermolecular interactions of NDIs could be directed and/or promoted by the display of such species as side chains of cyclic

ghadiri@scripps.edu.

<sup>[a]</sup>These authors contributed equally to this work.

D,L  $\alpha$ -peptides. It was envisioned that controlling aromatic ring interactions and geometry through peptide backbone directed self-assembly<sup>[17]</sup> might provide a rational supramolecular approach to conductive materials engineering. Towards these goals, in the studies reported here we present a model system for probing hydrogen bond directed intermolecular NDI-NDI interactions in solution. We report the methods developed for the synthesis of NDI modified cyclic D,L  $\alpha$ -peptides, examine their propensity for self-assembly by NMR, and probe the efficiency of intermolecular NDI-NDI charge transfer by fluorescence measurements.

## Results and Discussion

### Design

Cyclic D,L  $\alpha$ -peptides can form cylindrical  $\beta$ -sheet ensembles through hydrogen bond directed ring stacking.<sup>[2]</sup> Interrupting the hydrogen bonding network on one face of the cyclic peptide subunit through backbone N-alkylation restricts the self-assembly to antiparallel cylindrical dimers (Figure 1a).<sup>[18, 19]</sup> Such assemblies represent the asymmetric unit of the parent extended peptide nanotube and have proven to be useful models for probing the nanotube structure, self-assembly process, and functional properties.<sup>[10a, 17–20]</sup> We have used this strategy here to investigate the design and optical properties of NDI functionalized self-assembling cyclic D,L  $\alpha$ -peptides.

Modeling suggests that NDI modified side chains could adopt productive charge transfer geometries in the context of the cyclic D,L  $\alpha$ -peptide dimer (Figure 1b, c). Accordingly, peptides **1–5** (Figure 2) were designed in order to probe the influence of linker length, distal NDI substituent, and number of NDI amino acid side chains on the dimer self-assembly and optical properties. Peptides **1–3**, which bear a single NDI side chain, were designed to evaluate the effects of steric bulk of the distal NDI substituent (methyl in **3** vs. isobutyl in **1** and **2**). The effect of linker length was examined by comparing properties of cylindrical dimers derived from peptides **1** and **2**. Peptides **4** and **5**, which bear two NDI side chain functionalities, were designed similarly to examine the role of multiple NDI substitutions and linker length. It should be noted that ring symmetry is an important design consideration in these molecules as it determines the number of non-equivalent dimeric assemblies that a given cyclic peptide can form.<sup>[17, 19]</sup> In the flat ring conformation adopted by an eight residue cyclic D,L  $\alpha$ -peptide in the context of a nanotube, the backbone is  $C_4$  symmetric with the axis of rotation perpendicular to the plane of the ring.<sup>[2b, 19]</sup> Accordingly, the dimer shown in Figure 1a depicts only one of four possible diastereomeric assemblies which differ in the cross-strand pairing of homochiral amino acids. Depending on the peptide sequence, one or more of these dimers may be equivalent. Therefore, the  $C_1$  symmetric peptides **1–3** can each form four different diastereomeric assemblies (Figure 1d), whereas the  $C_2$  symmetric eight residue peptides **4** and **5** can form a maximum of two diastereomers. This is an important consideration as inter-subunit NDI-NDI interactions should only be possible in dimeric species where the aromatic side chains are juxtaposed across each other on opposite rings.

### Synthesis

We investigated three synthetic routes toward the desired cyclic peptides bearing NDI side chains. These include preparation from an NDI functionalized amino acid<sup>[21]</sup>, post-synthetic modification<sup>[16c]</sup> of cyclic D,L  $\alpha$ -peptides (Scheme 2), and modification of natural amino acid side chains during the course of solid phase peptide synthesis<sup>[22]</sup> (Scheme 3). We found for the synthesis of peptides **1–5**, the latter approach to be most general and synthetically convenient. Central to each of these approaches is the preparation of unsymmetrically substituted NDIs. Symmetrical NDIs such as N,N'-dibutyl-1,4,5,8-naphthalenetetracarboxylic diimide (**7**) can be prepared by condensation of 1,4,5,8-naphthalenetetracarboxylic dianhydride (**6**) with two equivalents of a primary amine (Scheme 1).<sup>[23]</sup> Unsymmetrical NDIs present a

greater challenge and have been typically prepared from anhydride **6** by condensation with a 1:1 mixture of two different primary amines, leading to a statistical mixture of products. We have found that a modification of a reported synthesis of NDI cyclophanes<sup>[24]</sup> to be a convenient alternative to this approach (Scheme 1). Following complete hydrolysis of a suspension of **6** (20 mM in water) with KOH, reacidification to pH 6.2 with H<sub>3</sub>PO<sub>4</sub> leads to the formation of the naphthalenetetracarboxylic monoanhydride diacid. Addition of one equivalent of a primary amine to the same reaction vessel followed by overnight refluxing yields naphthalene monoimides **8a–c** in good isolated yield and purity by a simple filtration workup.

We found that the dicarboxylic acid moieties in **8a–c** could be directly converted to imides by condensation with primary amines in DMF at temperatures above 110°C without the need to first isolate the corresponding anhydrides.<sup>[16c, 24]</sup> In one example of the use of monoimides (**8**) in the synthesis of cyclic D,L  $\alpha$ -peptides (Scheme 2), the four free amine lysine side chains of peptide **9** were converted to diimides by heating at 115°C with Cbz-ethylenediamine modified monoimide **8c** in DMF. Deprotection of the Cbz protecting groups followed by purification yielded tetra-NDI substituted peptide **10** in 38% overall yield for the two steps. Naphthalene monoimides were also incorporated onto peptides via on-resin conversion of lysine or ornithine side chain amines to imides (Scheme 3). A representative synthesis began with preparation of linear peptide **11** using standard Fmoc solid phase peptide synthesis protocols, employing  $\epsilon$ -4-methyltrityl (MTT) protected lysine. The resin bearing **11** was treated with dilute TFA to remove the MTT protecting group, and the resulting free amines converted to imides by stirring the resin with an excess of **8b** in DMF at 110°C. The NDI modified linear peptide was cleaved from the resin by treatment with TFA and purified by preparative HPLC to yield **12** in 28% overall yield. Treatment of **12** with (7-azabenzotriazole-1-yl)oxy tripyrrolidinophosphonium hexafluorophosphate (PyAOP) and diisopropylethylamine at 0.7 mM in DMF led to formation of the desired cyclic product **4** in 71% isolated yield. This synthetic approach was also used to prepare peptides **1**, **2**, **3**, and **5**.

### NMR Structural Characterization

NMR was utilized to probe the structure and assembly of peptides **1–5** in CDCl<sub>3</sub>. <sup>1</sup>HNMR spectra at low concentrations (~200  $\mu$ M) are sharp and consistent with the preponderance of monomeric species in solution. Spectra of peptides **4** and **5** showed peaks for only four different residues, indicating that these peptides maintain an apparent C<sub>2</sub> symmetry in solution. For each peptide, increasing the concentration leads to a new set of peaks consistent with hydrogen bonded dimeric species in slow exchange with the monomer on the NMR time scale.<sup>[19a]</sup> The concentration dependent monomer to dimer ratio was used to determine the apparent self-association constants ( $K_a$ ) (Table 1). In the calculation of the association constants, all possible diastereomeric ensembles formed by a given peptide were considered equivalent. Thus, the  $K_a$  values in Table 1 reflect the overall propensity for self-association demonstrated by each peptide. <sup>1</sup>HNMR data fit well to the self-association model, and the results of the calculations show that peptides form dimeric species with  $K_a$  ranging from 51 to 192 M<sup>-1</sup> in CDCl<sub>3</sub>.

Direct comparison of the association constants for the non-symmetric peptides **1–3** with that of the C<sub>2</sub> symmetric peptides **4** and **5** is complicated by two factors. The non-equivalent diastereomeric assemblies that can be formed from the dimerization of the peptide give rise to an entropy of mixing term that varies with the number and population of those assemblies.<sup>[25]</sup> In addition, a free energy term arising from the symmetry difference between the peptide monomer and dimer contributes a symmetry component to the observed  $K_a$  that is independent of the inherent chemical propensity to self-associate.<sup>[26]</sup> Performing calculations for the C<sub>1</sub> and C<sub>2</sub> symmetric peptides, however, shows that the energetic contribution from these two terms cancel assuming that a statistical mixture of dimeric assemblies is formed.

The differences in the binding constants of the various molecules provide some insight into the effect of the NDI modification on assembly of the peptide backbone. Comparison of the single NDI containing peptides **1** and **2** to the bis-NDI peptides **4** and **5**, respectively, show 2-fold decrease in the binding constants accompanying incorporation of an additional NDI side chain. This suggests that multiple NDIs on a cyclic peptide tend to destabilize dimer formation. Comparison of **4** to **5** and **1** to **2** show ~60% decrease in  $K_a$  for the lysine based linkers, indicating that the dimer is more stable when the NDI group is tethered closer to the peptide backbone. The similar association constants for **1** and **3** indicate that the distal NDI substituent has little impact on intermolecular peptide self-association.

### Fluorescence Characterization

Charge delocalization as a consequence of aromatic ring stacking provides the basis for the electronic properties observed in high order NDI aggregates. Charge transfer within an NDI dimer in solution leads to the formation of excimers that can be conveniently monitored by fluorescence spectroscopy.<sup>[27]</sup> Thus, the role of cyclic peptide backbone self-assembly in enhancing NDI-NDI interactions was probed through fluorescence measurements. Figure 3a shows the fluorescence spectra for single NDI containing peptides **1**, **2**, and **3** as well as the control compound **7** at 1.65 mM in CDCl<sub>3</sub>. The formation of excimers is indicated by the presence of a broad peak with a maximum at 492 nm, red shifted with respect to the monomeric peaks at wavelengths of 434 and 408 nm due to charge delocalization. As expected from the peptide self-assembly observed by NMR, all three peptides (**1–3**) show enhanced excimer peak intensity relative to the control compound **7**. These effects can be seen throughout the concentration range (0.1 – 5 mM) studied (Figure 3b).

Although the practical range of peptide concentration that can be studied (as determined by the magnitude of  $K_a$ ) is above where rigorous quantitative analysis of the fluorescence data is possible, some qualitative differences are clear. Differences in excimer peak intensity suggest that, in addition to the enhanced effective concentration brought about by peptide backbone directed self-assembly, other structural parameters seem to play a role in the formation of NDI excimers. It is evident that peptide **3** has a much higher propensity for the formation of NDI excimers than **1**. Since the NMR data show similar association constants for the two peptides, the difference in excimer formation can be attributed to the reduced steric hindrance from the distal NDI methyl group in **3** versus the branched isobutyl moiety in **1** allowing more productive interactions between the aromatic rings.

The length of the tether between the peptide backbone and the NDI substituent seems to also influence NDI excimer formation. Peptide **1** shows an increase in excimer formation relative to the control compound **7**, while **2**, which has an association constant almost twice that of **1** by NMR, shows excimer peak intensity closer to that of the control compound. This suggests that the shorter ornithine based linker between the NDI and the cyclic peptide backbone in **2** does not allow the necessary flexibility for the NDI side chains to adopt an orientation on adjacent peptide strands suitable for an efficient charge transfer. In contrary to the effect of linker length on peptide dimerization, in this case the additional degrees of freedom offered by the lysine based linker allow more favorable intermolecular NDI interactions relative to the shorter ornithine.

As discussed above, in the non-symmetrically substituted peptide **3**, the dimer in which the NDI side chains are juxtaposed across from each other represents only one of four possible diastereomeric assemblies (Figure 1d). In calculation of the apparent association constants reported in Table 1, these dimers were all considered equivalent. It is reasonable to assume that only the assembly in which the NDI side chains overlap would be productive with respect to intermolecular excimer formation (Figure 1b, c). Yet, this dimer is likely the least stable and therefore least populated of the four, as the other three have the bulky NDI moiety paired with

less sterically demanding alanine side chains. Although peptides **4** and **5** show  $K_a$  two orders of magnitude larger than that of **7** by NMR, efforts to probe the efficiency of the intermolecular NDI charge transfer in these  $C_2$  symmetric peptides were not informative due to interference by intramolecular NDI interactions. The fluorescence spectrum of each exhibits a large concentration independent excimer peak (data not shown). This peak remains even at concentrations where the  $^1\text{H}$ NMR indicates that only monomers exist in solution for both peptides, suggesting that there is enough flexibility in the peptide backbone to allow productive intramolecular interaction between NDI side chains. As expected, this intramolecular NDI excimer formation depends on linker length and is more pronounced in **4** than **5**.

In conclusion, the above studies indicate that cyclic D,L  $\alpha$ -peptide self-assembly can be an effective process for templating directed aromatic side chain-side chain interactions. It is therefore expected that the design rationale described here coupled with the efficient synthetic process should allow access to a variety of cyclic D,L  $\alpha$ -peptide sequences bearing NDI side chains for use in the construction of self-assembling peptide nanotube analogs with novel optical and electronic properties.

## Experimental Section

**General**—The Fmoc-amino acids, resins used for solid phase peptide synthesis, and 2-(1H-benzotriazole-1-yl)-1,1,3,3-tetramethyluronium hexafluorophosphate (HBTU) were all purchased from Novabiochem. NMR solvents were obtained from Cambridge Isotope Labs. N-Cbz-ethylene-diamine-hydrochloride was purchased from TCI America. (7-azabenzotriazole-1-yloxy) tripyrrolidinophosphonium hexafluorophosphate (PyAOP) and all other solvents and reagents were purchased from Aldrich. DMF used in coupling and cyclization steps was dried over 4 Å molecular sieves. All other reagents and solvents were used as received. Reverse phase HPLC was carried out on  $C_{18}$  columns using gradients between 99 : 1 : 0.1 (water/acetonitrile/TFA) and 10 : 90 : 0.1 (water/acetonitrile/TFA). NMR spectra were obtained on Bruker AMX-400, DRX-500, or DRX-600 spectrometers. UV-VIS measurements were made on a Cary 100 Bio UV-visible Spectrophotometer. Fluorescence spectra were acquired on an Aminco Bowman Series 2 Luminescence Spectrometer.

**Monoimide 8a**—1,4,5,8-naphthalenetetracarboxylic dianhydride (**6**) (2.0 g, 7.46 mmol) was weighed into a 500-ml flask. Water (350 ml) was added, followed by 1 M KOH (35 ml). In some cases, heat, sonication, and/or additional KOH was used to completely dissolve the starting material. After the solid dissolved, the solution was acidified to pH 6.4 with 1 M  $\text{H}_3\text{PO}_4$ . Isobutylamine (0.741 ml, 7.46 mmol) was added, and the solution was again acidified to pH 6.4 with 1 M  $\text{H}_3\text{PO}_4$ . The reaction vessel was fitted with a reflux condenser, heated to 110 °C, and stirred overnight. The reaction was then cooled to room temperature and filtered. Acetic acid (5 ml) was added to the filtrate and a white solid precipitated from the solution. The solid was collected by filtration, washed with water, and dried under high vacuum to yield 1.714 g (67%) of the desired product as an off-white solid.  $^1\text{H}$ NMR (400MHz,  $\text{DMSO-d}_6$ ):  $\delta$  8.51 (d,  $J = 7$  Hz, 2H), 8.07 (d,  $J = 7$  Hz, 2H), 3.90 (d,  $J = 7$  Hz, 2H), 2.12 (m, 1H), 0.90 (d,  $J = 7$  Hz, 6H);  $^{13}\text{C}$ NMR (100MHz,  $\text{DMSO-d}_6$ ):  $\delta$  169.7, 163.3, 130.3, 128.6, 128.1, 128.0, 125.5, 123.4, 46.6, 26.9, 20.2; MALDI-FTMS:  $[\text{M}+\text{H}]^+$  obsd. = 342.0972 (calc. = 342.0964).

**Monoimide 8b**—Prepared by the reaction of 1,4,5,8-naphthalenetetracarboxylic dianhydride (**6**) (1.0 g, 3.73 mmol) with methylamine-hydrochloride (252 mg, 3.73 mmol) as described for **8a**. The reaction yielded 890 mg (80%) of the product as a pale yellow solid.  $^1\text{H}$ NMR (500 MHz,  $\text{D}_2\text{O}$ ):  $\delta$  8.56 (d,  $J = 8$  Hz, 2H), 8.05 (d,  $J = 8$  Hz, 2H), 3.47 (s, 3H);  $^{13}\text{C}$ NMR (125 MHz,  $\text{NaOD/D}_2\text{O}$ , DSS as internal standard):  $\delta$  178.0, 169.1, 147.6, 134.0, 131.6, 129.5, 127.5, 124.8, 29.6; ESI-TOF MS:  $[\text{M}-\text{H}]^-$  obsd. = 298.0360 (calc. = 298.0357).



**Monoimide 8c**—Prepared by the reaction of 1.163 g (4.34 mmol) of 1,4,5,8-naphthalenetetracarboxylic dianhydride (**6**) with 1.0 g (4.33 mmol) N-Cbz-ethylene-diamine-hydrochloride as described for **2a**. The reaction yielded 1.129 g (56%) of the product as a pale tan solid. <sup>1</sup>HNMR (400 MHz, DMSO-d<sub>6</sub>) δ 8.50 (d, *J* = 8 Hz, 2H), 8.07 (d, *J* = 8 Hz, 2H), 7.4–7.2 (m, 6H), 4.94 (s, 2H), 4.16 (t, *J* = 6 Hz, 2H), 3.60 (q, *J* = 6 Hz, 2H); <sup>13</sup>CNMR (150 MHz, DMSO-d<sub>6</sub> with 4 eq. triethylamine to improve solubility) δ 170.8, 163.6, 156.2, 146.3, 137.2, 129.9, 128.7, 128.1, 127.5, 127.4, 126.3, 125.7, 121.6, 64.9, 38.2; ESI-TOF MS (m/z) [M-H]<sup>-</sup> obsd. = 461.0989 (calc. = 461.0990).

**Cyclic Peptide 9**—Peptide **9** was prepared from Fmoc-Lys-OAllyl attached via the amine of the lysine side chain to 2-Cl-Trt resin using methodology previously reported.<sup>[28]</sup> The crude material was purified by preparative RP-HPLC. ESI-TOF MS (m/z) [M+H]<sup>+</sup> obsd. = 1561.9134 (calc. = 1561.9141).

**NDI derivitization of a peptide in solution – Synthesis of 10**—Peptide **9** (11 mg, 5.5 μmol assuming a salt with 4 molecules of trifluoroacetate per peptide) and **8c** (12.6 mg, 27.3 μmol) were suspended in DMF (5 ml). The mixture was heated to 115 °C under argon and stirred overnight. The resulting solution was cooled to room temperature and concentrated to dryness. The remaining solid was washed (2 × 2 ml) with pH 8.0 phosphate buffer, the supernatant discarded, and the solid dried under high vacuum. The crude solid was dissolved in 10:2:2 TFA/trimethylsilyl trifluoromethanesulfonate/*m*-cresol (200 μl). After 1 hr, ether (2 ml) was added, and the resulting suspension centrifuged. The supernatant was discarded, and the solid washed twice more with ether (2 ml). The crude peptide was purified by preparative RP-HPLC to yield 6.4 mg (38% assuming a salt with 8 molecules of trifluoroacetate per peptide) of the product as an off white solid. <sup>1</sup>HNMR (600 MHz, CDCl<sub>3</sub>/TFA, all signals were broad, likely due to aggregation; integration of amide NH at 6.93 ppm was lower than 8 due to partial exchange with TFA) δ 8.93 (br s, 16H), 6.93 (br s, 7 H), 4.91 (br s, 8 H), 4.79 (br s, 8 H), 4.31 (br s, 8H), 3.82 (br s, 8H), 3.37 (br s, 8H), 2.00 (br s, 32 H), 1.65 (br s, 16H); ESI-TOF MS (m/z) [M+2H]<sup>2+</sup> obsd. = 1097.4841 (calc. = 1097.4840).

### Representative on-resin NDI derivitization of peptides – Synthesis of 12

**1. Protected linear peptide on resin**—Fmoc-Lys(MTT) Wang polystyrene resin (139 mg, 0.100 mmol) was weighed into a sintered glass peptide synthesis vessel and allowed to swell in CH<sub>2</sub>Cl<sub>2</sub> for 45 min, then in DMF for 10 min. The resin was treated with 20% piperidine/DMF (2 x 8 min) to remove the Fmoc group, and washed with DMF (3x). A solution of Fmoc-D-leucine (142 mg, 0.40 mmol), HBTU (148 mg, 0.39 mmol), and diisopropylethylamine (175 μl, 1.0 mmol) in DMF (3 ml) was allowed to prereact for 2 min then added to the resin. The resin suspension was agitated for 30 min, drained, and washed with DMF (3x). This deprotection – coupling cycle was repeated to obtain the full length linear peptide **11**. Coupling reactions following *N*-methyl-alanine residues were performed twice to ensure complete reaction.

**2. Conversion of Resin bound Lys(MTT) to Lys(NDI) and cleavage from resin**—The resin bearing **11** was washed with CH<sub>2</sub>Cl<sub>2</sub> (3 x 1 min) and treated with a mixture of 93 : 5 : 2 CH<sub>2</sub>Cl<sub>2</sub>/triethylsilane/trifluoroacetic acid (3 x 2 min followed by 3 x 10 min) to remove the lysine MTT protecting groups. The resin was then washed sequentially with CH<sub>2</sub>Cl<sub>2</sub>, DMF, 95:5 DMF/disopropylethylamine, and again with DMF. The resin was transferred to a 20 ml vial to which **8a** (1.5 eq relative to resin bound amines, 102 mg, 0.30 mmol) was added followed by DMF (8 ml). The suspension was heated to 110 °C and stirred for 6 hr. The reaction was cooled to room temperature, and filtered through a fritted syringe. The resin was washed thoroughly (5 x DMF, 3 x CH<sub>2</sub>Cl<sub>2</sub>, 3 x MeOH) and dried under high vacuum. The peptide was cleaved from the resin by treatment with 95:5 TFA/H<sub>2</sub>O for 3 hr. The cleavage mixture was

collected by filtration and the resin was washed twice with TFA. The filtrates were combined and concentrated under vacuum to an oily residue. Water was added and the mixture was sonicated to produce a suspension of cream colored solid. This mixture was frozen and lyophilized to yield crude product. Purification by preparative RP-HPLC on a C<sub>18</sub> column yielded 46 mg (28%) of the trifluoroacetate salt of the product as an off-white solid. MALDI-FTMS: [M+H]<sup>+</sup> obsd. = 1507.7926 (calc. = 1507.7871).

**Cyclic 4**—Linear peptide **12** (46 mg, 28 μmol) was dissolved in DMF (40 ml). PyAOP (44 mg, 85 μmol) was added followed by diisopropylethylamine (30 μl, 170 μmol). The reaction was stirred for 2.5 hr at room temperature and concentrated under vacuum. Water/acetonitrile/TFA (8 ml of 1 : 1 : 0.001) was added and the residue was sonicated to create a suspension. After centrifugation, the supernatant was removed. The solid was washed twice more with the same procedure. The resulting pellet was suspended in water, sonicated, and lyophilized to yield 30 mg (71%) of the product as an off white solid. <sup>1</sup>HNMR (600 MHz, CDCl<sub>3</sub>): δ 8.55 (s, 8H), 7.59 (d, *J* = 8 Hz, 2H), 6.82 (d, *J* = 10 Hz, 2H), 6.55 (d, *J* = 7 Hz, 2H), 5.25 (q, *J* = 7 Hz, 2H), 4.87 (dd, *J* = 7, 8 Hz, 2H), 4.65 (dd, *J* = 6, 6 Hz, 2H), 4.46 (dt, *J* = 4, 10 Hz, 2H), 4.10 (m, 4H), 4.00 (d, *J* = 7 Hz, 4H), 2.83 (s, 6H), 2.19 (m, 2H), 1.96 (m, 2H), 1.9–1.7 (m, 8H), 1.68–1.36 (m, obscured by H<sub>2</sub>O), 1.32 (d, *J* = 7 Hz, 6H), 0.97–0.93 (overlapping doublets, 24H), 0.90 (d, *J* = 7 Hz, 6H), 0.85 (d, *J* = 7 Hz, 6H); MALDI-FTMS: [M+H]<sup>+</sup> obsd. = 1489.7760 (calc. = 1489.7766).

**Linear precursor to 1**—Linear peptide was synthesized from Fmoc-Ala Wang polystyrene resin (141 mg, 0.10 mmol) and purified as described above for **12** to yield 27 mg (21%) of the trifluoroacetate salt of the product as a white solid. MALDI-FTMS: [M+H]<sup>+</sup> obsd. = 1145.6621 (calc. = 1145.6605).

**Cyclic 1**—Linear precursor (27 mg, 21.4 μmol) was cyclized as described for **4**. The product was purified by RP-HPLC on a C<sub>18</sub> column to yield 12 mg (50%) of the desired product as a white solid. <sup>1</sup>HNMR (600 MHz, CDCl<sub>3</sub>): δ 8.75(d, *J* = 2 Hz, 4H), 7.58 (d, *J* = 8 Hz, 1H), 7.51 (d, *J* = 9 Hz), 6.86 (d, *J* = 9 Hz, 1H), 6.80 (d, *J* = 10 Hz, 1H), 6.66 (d, *J* = 6 Hz, 1H), 6.57 (d, *J* = 7 Hz, 1H), 5.24 (m, 2H), 4.85 (m, 2H), 4.59 (m, 2H), 4.46 (m, 2H), 4.15 (t, *J* = 8 Hz, 2H), 4.06 (d, *J* = 7 Hz, 2H), 2.82 (overlapping s, 6H), 2.23 (m, 1H), 1.37 (d, *J* = 7 Hz, 3H), 1.32 (d, *J* = 7 Hz, 6H), 1.95–1.40 (m, obscured by H<sub>2</sub>O), 1.0–0.8 (overlapping d, 30H); MALDI-FTMS: [M+Na]<sup>+</sup> obsd. = 1149.6313 (calc. = 1149.6319).

**Linear precursor to 2**—Linear peptide was synthesized from Fmoc-Ala Wang polystyrene resin (141 mg, 0.10 mmol) and purified as described above for **12** to yield 8 mg (6%) of the trifluoroacetate salt of the product as a white solid. MALDI-FTMS: [M+H]<sup>+</sup> obsd. = 1131.6441 (calc. = 1131.6448).

**Cyclic 2**—Linear precursor (8 mg, 6.4 μmol) was cyclized as described for **4**. The product was purified by RP-HPLC on a C<sub>18</sub> column to yield 4.2 mg (59%) of the desired product as an off-white solid. <sup>1</sup>HNMR (600 MHz, CDCl<sub>3</sub>): δ 8.75 (d, *J* = 8 Hz, 2H), 8.72 (d, *J* = 8 Hz, 2H), 7.61 (d, *J* = 7 Hz, 1H), 7.46 (d, *J* = 8 Hz, 1H), 6.83 (d, *J* = 9 Hz, 1H), 6.77 (d, *J* = 8 Hz, 1H), 6.66 (br s, 1H), 6.57 (br s, 1H), 5.21 (br s, 2H), 4.83 (m, 2H), 4.66 (m, 1H), 4.56 (m, 1H), 4.48 (m, 1H), 4.44 (m, 1H), 4.15 (m, 2H), 4.06 (d, *J* = 8 Hz, 2H), 2.28 (s, 6H), 2.0–1.2 (overlapping multiplets obscured by H<sub>2</sub>O peak), 1.35 (d, *J* = 7 Hz, 3H), 1.31 (d, *J* = 7 Hz, 6H), 1.0–0.87 (overlapping doublets, 36H); MALDI-FTMS: [M+H]<sup>+</sup> obsd. = 1113.6343 (calc. = 1113.6343).

**Linear precursor to 3**—Linear peptide was synthesized (using monoimide **8b**) from Fmoc-Ala Wang polystyrene resin (141 mg, 0.10 mmol) and purified as described above for **12** to

yield 16 mg (13%) of the trifluoroacetate salt of the product as a white solid. MALDI-FTMS:  $[M+H]^+$  obsd. = 1103.6113 (calc. = 1103.6135).

**Cyclic 3**—Linear precursor (16 mg, 13.1  $\mu\text{mol}$ ) was cyclized as described for **4**. The product was purified by RP-HPLC on a  $C_{18}$  column to yield 8 mg (56%) of the desired product as an off-white solid.  $^1\text{H NMR}$  (600 MHz,  $\text{CDCl}_3$ )  $\delta$  8.76 (s, 4H), 7.57 (d,  $J = 8$  Hz, 1H), 7.49 (d,  $J = 8$  Hz, 1H), 6.85 (d,  $J = 10$  Hz, 1H), 6.79 (d,  $J = 10$  Hz, 1H), 6.63 (d,  $J = 6$  Hz, 1H), 6.55 (d,  $J = 7$  Hz, 1H), 5.24 (m, 2H), 4.86 (m, 2H), 4.59 (m, 2H), 4.46 (m, 2H), 4.15 (t,  $J = 8$  Hz, 2H), 3.59 (s, 3H), 2.82 (s, 3H), 2.81 (s, 3H), 1.9–1.4 (overlapping multiplets), 1.36 (d,  $J = 7$  Hz, 3H), 1.31 (d,  $J = 7$  Hz, 6H), 1.23 (s, 3H), 0.98–0.84 (overlapping doublets, 24H); ESI-TOF MS:  $[M+H]^+$  obsd. = 1085.6030 (calc. = 1085.6030).

**Linear precursor to 5**—Linear peptide was synthesized from Fmoc-Orn(MTT) Wang polystyrene resin (204 mg, 0.10 mmol) and purified as described above for **12** to yield 39 mg (24%) of the trifluoroacetate salt of the product as a white solid. MALDI-FTMS:  $[M+H]^+$  obsd. = 1479.7511 (calc. = 1479.7558).

**Cyclic 5**—Linear precursor (39 mg, 24.4  $\mu\text{mol}$ ) was cyclized as described for **4** to yield 33 mg (93%) of the product as an off-white solid.  $^1\text{H NMR}$  (500 MHz,  $\text{CDCl}_3$ ):  $\delta$  8.70 (s, 8H), 7.55 (d,  $J = 8$  Hz, 2H), 6.78 (d,  $J = 10$  Hz, 2H), 6.55 (d,  $J = 7$  Hz, 2H), 5.21 (q,  $J = 7$  Hz, 2H), 4.84 (dd,  $J = 7, 8$  Hz, 2H), 4.72 (dd,  $J = 6, 6$  Hz, 2H), 4.47 (td,  $J = 10, 4$  Hz), 4.19 (m, 4H), 4.04 (d,  $J = 7$  Hz, 4H), 2.81 (s, 6H), 2.2 (m, 2H), 1.98 (m, 2H), 1.85–1.40 (m, 18H), 1.30 (d,  $J = 7$  Hz, 6H), 0.98 (d,  $J = 7$  Hz, 12H), 0.92 (m, 24H); MALDI-FTMS:  $[M+Na]^+$  obsd. = 1483.7228 (calc. = 1483.7272).

**Concentration Dependent NMR for *N*-Me cyclic peptides**—<sup>[19a]</sup> All spectra were obtained in  $\text{CDCl}_3$  (99.96% from Cambridge Isotope Labs). A stock solution of freshly dried peptide was made in  $\text{CDCl}_3$ , and this solution was sonicated and centrifuged to remove any insoluble material. The concentration of this stock was determined by absorption spectroscopy ( $\text{NDI } \epsilon_{380} = 29,850 \text{ cm}^{-1} \cdot \text{M}^{-1}$ ). The stock solution was then diluted to make samples at the desired concentrations (at least three different concentrations for each peptide).  $^1\text{H NMR}$  spectra were obtained on a Bruker DRX-500 or DRX-600 spectrometer. As the monomer and dimer species are in slow exchange on the NMR time scale, peaks were visible for both species. The data were fit to the following model:

$$K = \frac{[A_2]}{[A]^2} \quad [1]$$

and

$$C_{tot} = 2[A_2] + [A] \quad [2]$$

where  $[A]$  and  $[A_2]$  are the concentrations of monomer and dimer respectively and  $C_{tot}$  is the total concentration. The integrated intensities of the backbone *N*-methyl groups were used to measure the ratio of the two species. A variable  $x$  was defined according to eq 3:

$$x \equiv \frac{I_{dimer}}{2I_{monomer}} = \frac{[A_2]}{[A]} \quad [3]$$

where  $I_{dimer}$  is the integrated intensity of dimer *N*-methyl peaks and  $I_{monomer}$  is the integrated intensity of monomer *N*-methyl peaks. Combining equations 1–3 gives eq. 4.



$$C_{tot} = \frac{2x^2 + x}{K} \quad [4]$$

The equilibrium constant for dimerization ( $K$ ) was found from the inverse of the slope of the linear fit of  $C_{tot}$  against  $(2x^2+x)$  for each experimental concentration.

**Self-association constant of 7 by NMR**—<sup>[29]</sup> NDI control compound **7** demonstrated concentration dependent chemical shifts in the range of 1 to 50 mM. This concentration dependent behavior was modeled as a monomer and dimer in equilibrium and in fast exchange on the NMR time scale. The data was modeled using the self-association equilibrium shown in equations 1 and 2 described above. For a given  $C_{tot}$  and an arbitrary value of  $K$ ,  $[A]$  can be found from the root of eq. 5

$$2[A]^2K + [A] - C_{tot} = 0 \quad [5]$$

where  $[A]$  is greater than 0 and less than  $C_{tot}$ . Assuming equilibrium between monomer and dimer in fast exchange, the chemical shift for a given proton in **7** follows eq [6]

$$\delta = \frac{2K[A]^2}{C_{tot}}(\delta_2 - \delta_1) + \delta_1 \quad [6]$$

where  $\delta$  is the observed chemical shift,  $\delta_1$  is the chemical shift of the monomer, and  $\delta_2$  is the chemical shift of the dimer. Thus, observed  $\delta$  for each experimental  $C_{tot}$  are used with an arbitrary  $K$  in eq. [7]

$$\frac{2K[A]^2}{C_{tot}} \quad [7]$$

to determine  $\delta_1$  and  $\delta_2$  by linear regression analysis. These values are used, in turn, to calculate a theoretical  $\delta$  for each experimental concentration. Numerical minimization of the sum of the squares of the residuals between observed and calculated  $\delta$  gave the best fit when  $K = 0.44 \text{ M}^{-1}$ .

**Fluorescence Measurements**—Stock solutions were prepared in  $\text{CDCl}_3$  as described above for the concentration dependent NMR experiments. Samples were measured in a  $0.2 \times 1 \text{ cm}$  quartz cuvette ( $0.2 \text{ cm}$  along excitation path). The excitation wavelength was  $330 \text{ nm}$  and the detector voltage was kept the same for all samples.

#### Acknowledgements

We would like to thank the National Institute of Health (GM52190) and the Air Force Office of Scientific Research (F49620-00-1-0283) for financial support. W.S.H. thanks the National Science Foundation for a Predoctoral Fellowship and N.A. the Fulbright Foundation for a Postdoctoral Fellowship.

#### References

1. For a review, see: Bong DT, Clark TD, Granja JR, Ghadiri MR. *Angew Chem* 2001;113:1016–1041. *Angew Chem Int Ed* 2001;40:988–1011.
2. Cyclic D,L  $\alpha$ -peptides: a) Ghadiri MR, Granja JR, Milligan RA, McRee DE, Khazanovich N. *Nature* 1993;366:324–327. [PubMed: 8247126] b) Hartgerink JD, Granja JR, Milligan RA, Ghadiri MR. *J Am Chem Soc* 1996;118:43–50. c) Rosenthal-Aizman K, Svensson G, Uden A. *J Am Chem Soc* 2004;126:3372–3373. [PubMed: 15025434]

3. Cyclic  $\beta$ -peptides: a) Clark TD, Buehler LK, Ghadiri MR. *J Am Chem Soc* 1998;120:651–656. b) Seebach D, Matthews JL, Meden A, Wessels T, Baerlocher C, McCusker LB. *Helv Chim Acta* 1997;80:173–182.
4. Cyclic  $\alpha,\beta$ -peptides: Karle IL, Handa BK, Hassall CH. *Acta Crystallogr* 1975;B31:555–560.
5. Cyclic  $\alpha,\gamma$ -peptides: Amarin M, Castedo L, Granja JR. *J Am Chem Soc* 2003;125:2844–2845. [PubMed: 12617629]
6. Cyclic  $\delta$ -peptides: Gauthier D, Baillargeon P, Drouin M, Dory YL. *Angew Chem* 2001;113:4771–4774. *Angew Chem Int Ed* 2001;40:4635–4638.
7. Cyclic oligoureas: a) Ranganathan D, Lakshmi C, Karle IL. *J Am Chem Soc* 1999;121:6103–6107. b) Semetey V, Didierjean C, Briand J-P, Aubry A, Guichard G. *Angew Chem* 2002;114:1975–1978. *Angew Chem Int Ed* 2002;41:1895–1898.
8. Cyclic  $\alpha,\epsilon$ -peptides Horne WS, Stout CD, Ghadiri MR. *J Am Chem Soc* 2003;125:9372–9376. [PubMed: 12889966]
9. a) Ghadiri MR, Granja JR, Buehler LK. *Nature* 1994;369:301–304. [PubMed: 7514275] b) Granja JR, Ghadiri MR. *J Am Chem Soc* 1994;116:10785–10786. c) Sanchez-Quesada J, Isler MP, Ghadiri MR. *J Am Chem Soc* 2002;124:10004–10005. [PubMed: 12188661] d) Sanchez-Quesada J, Kim HS, Ghadiri MR. *Angew Chem* 2001;113:2571–2574. *Angew Chem Int Ed* 2001;40:2503–2506. e) Fernandez-Lopez S, Kim HS, Choi EC, Delgado M, Granja JR, Khasanov A, Kraehenbuehl K, Long G, Weinberger DA, Wilcoxon KM, Ghadiri MR. *Nature* 2001;412:452–456. [PubMed: 11473322]
10. a) Vollmer MS, Clark TD, Steinem C, Ghadiri MR. *Angew Chem* 1999;111:1703–1706. *Angew Chem Int Ed* 1999;38:1598–1601. b) Steinem C, Janshoff A, Vollmer MS, Ghadiri MR. *Langmuir* 1999;15:3956–3964. c) Motesharei K, Ghadiri MR. *J Am Chem Soc* 1997;119:11306–11312.
11. a) Bachtold A, Hadley P, Nakanishi T, Dekker C. *Science* 2001;294:1317–1320. [PubMed: 11588220] b) Collier CP, Mattern G, Wong EW, Luo Y, Beverly K, Sampaio J, Raymo FM, Stoddart JF, Heath JR. *Science* 2000;289:1172–1175. [PubMed: 10947980] c) Huang Y, Duan X, Wei Q, Lieber CM. *Science* 2001;291:630–633. [PubMed: 11158671] d) Joachim C, Gimzewski JK, Aviram A. *Nature* 2000;408:541–548. [PubMed: 11117734] e) Tour JM. *Acc Chem Res* 2000;33:791–804. [PubMed: 11087316]
12. a) Carloni P, Andreoni W, Parrinello M. *Phys Rev Lett* 1997;79:761–764. b) Jishi RA, Braier NC, White CT, Mintmire JW. *Phys Rev B* 1998;58:R16009–R16011. c) Lewis JP, Pawley NH, Sankey OF. *J Phys Chem B* 1997;101:10576–10583. d) Okamoto H, Nakanishi T, Nagai Y, Kasahara M, Takeda K. *J Am Chem Soc* 2003;125:2756–2769. [PubMed: 12603165] e) Okamoto H, Takeda K, Shiraishi K. *Phys Rev B* 2001;64:115425/1–115425/17.
13. a) Pope MS. *Wenberg CEElectronic Processes in Organic Crystals and Polymers Oxford Science Publications Oxford 1999* or recent examples see: b) Percec V, Glodde M, Bera TK, Miura Y, Shiyonovskaya I, Singer KD, Balagurusamy VSK, Heiney PA, Schnell I, Rapp A, Spiess HW, Hudson SD, Duan H. *Nature* 2002;419:384–387. [PubMed: 12352988] c) Schmidt-Mende L, Fechtenkotter A, Mullen K, Moons E, Friend RH, MacKenzie JD. *Science* 2001;293:1119–1122. [PubMed: 11498585]
14. Rapaport H, Kim HS, Kjaer K, Howes PB, Cohen S, Als-Nielsen J, Ghadiri MR, Leiserowitz L, Lahav M. *J Am Chem Soc* 1999;121:1186–1191.
15. a) Katz HE, Johnson J, Lovinger AJ, Li W. *J Am Chem Soc* 2000;122:7787–7792. b) Katz HE, Lovinger AJ, Johnson J, Kloc C, Slegrist T, Li W, Lin YY, Dodabalapur A. *Nature* 2000;404:478–481. [PubMed: 10761911]
16. a) Miller LL, Mann KR. *Acc Chem Res* 1996;29:417–423. b) Miller LL, Duan RG, Tully DC, Tomalia DA. *J Am Chem Soc* 1997;119:1005–1010. c) Tabakovic I, Miller LL, Duan RG, Tully DC, Tomalia DA. *Chem Mater* 1997;9:736–745.
17. Bong DT, Ghadiri MR. *Angew Chem* 2001;113:2221–2224. *Angew Chem Int Ed* 2001;40:2163–2166.
18. Hexameric, D,L  $\alpha$ -peptides Saviano M, Zaccaro L, Lombardi A, Pedone C, Di Blasio B, Sun X, Lorenzi GP. *J Inclusion Phenom* 1994;18:27–36.
19. Octameric D,L  $\alpha$ -peptides: a) Clark TD, Buriak JM, Kobayashi K, Isler MP, McRee DE, Ghadiri MR. *J Am Chem Soc* 1998;120:8949–8962. b) Ghadiri MR, Kobayashi K, Granja JR, Chadha RK, McRee DE. *Angew Chem* 1995;107:76–78. *Angew Chem Int Ed Engl* 1995;34:93–95.

20. a) Clark TD, Ghadiri MR. *J Am Chem Soc* 1995;117:12364–12365. b) Clark TD, Kobayashi K, Ghadiri MR. *Chem Eur J* 1999;5:782–792. c) Kobayashi K, Granja JR, Ghadiri MR. *Angew Chem Int Ed Engl* 1995;34:95–98. *Angew. Chem.* 1995, 107, 79–82
21. Wagner T, Davis WB, Lorenz KB, Michel-Beyerle ME, Diederichsen U. *Eur J Org Chem* 2003:3673–3679.
22. Mokhir AA, Kraemer R. *Bioconjugate Chem* 2003;14:877–883.
23. Sep WJ, Verhoeven JW, De Boer TJ. *Tetrahedron* 1975;31:1065–1070.
24. Buncel E, Mailloux NL, Brown RS, Kazmaier PM, Dust J. *Tetrahedron Lett* 2001;42:3559–3562.
25. Eliel, EL.; Wilen, SH.; Mander, LN. *Stereochemistry of Organic Compounds*. John Wiley & Sons; New York: 1994.
26. Benson SW. *J Am Chem Soc* 1958;80:5151–5154.
27. Barros TC, Brochsztain S, Toscano VG, Berci Filho P, Politi MJ. *J Photochem Photobiol, A* 1997;111:97–104.
28. a) Kates SA, Sole NA, Johnson CR, Hudson D, Barany G, Albericio F. *Tetrahedron Lett* 1993;34:1549–1552. b) Redman JE, Wilcoxon KM, Ghadiri MR. *J Comb Chem* 2003;5:33–40. [PubMed: 12523832]
29. Connors, KA. *Binding Constants: The Measurement of Molecular Complex Stability*. John Wiley & Sons; New York: 1987.

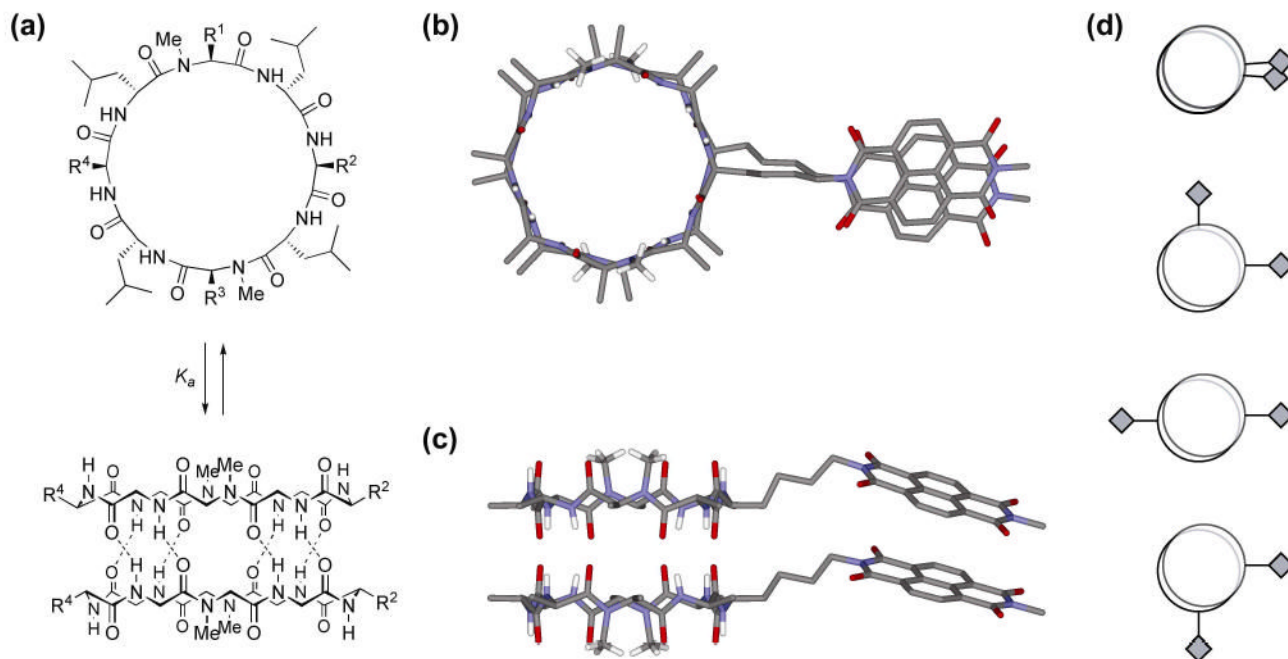


**Figure 1.**

(a) Schematic representation of hydrogen bond directed dimerization of backbone *N*-methylated cyclic D,L  $\alpha$ -peptides (for clarity most side chains are not depicted in dimeric assembly) with generic side chains  $R^1$ - $R^4$ ; (b) calculated model of one possible dimer of peptide 3 viewed from the top and (c) from the side (most side chains and protons omitted for clarity); (d) schematic illustration depicting overlap of NDI side chains (diamonds) in the four possible dimeric assemblies available to the  $C_1$  symmetric peptides 1, 2, and 3.

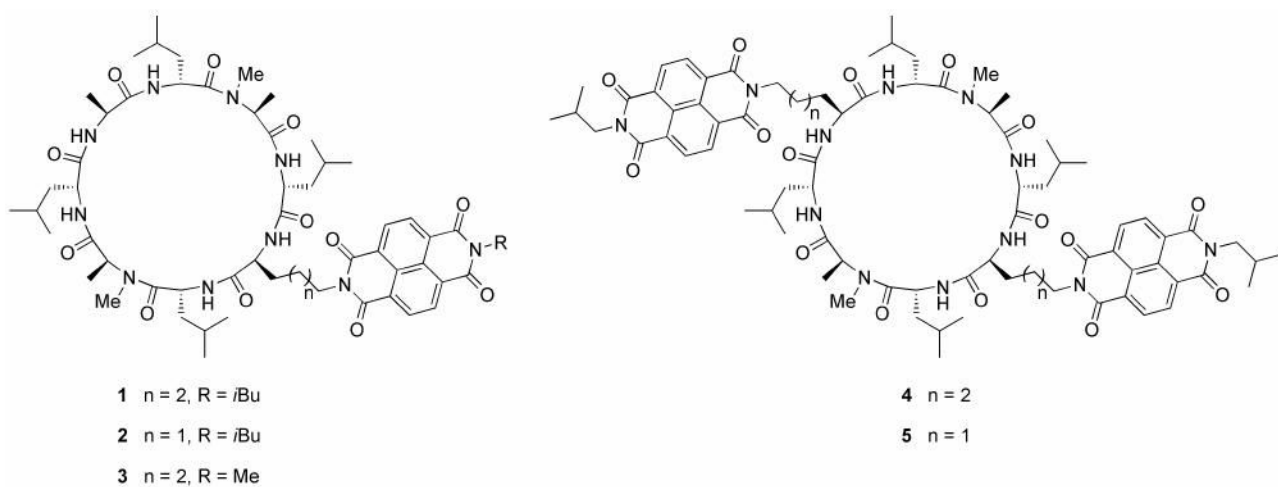


**Figure 2.**  
The NDI modified cyclic D,L α-peptide sequences used in this study.



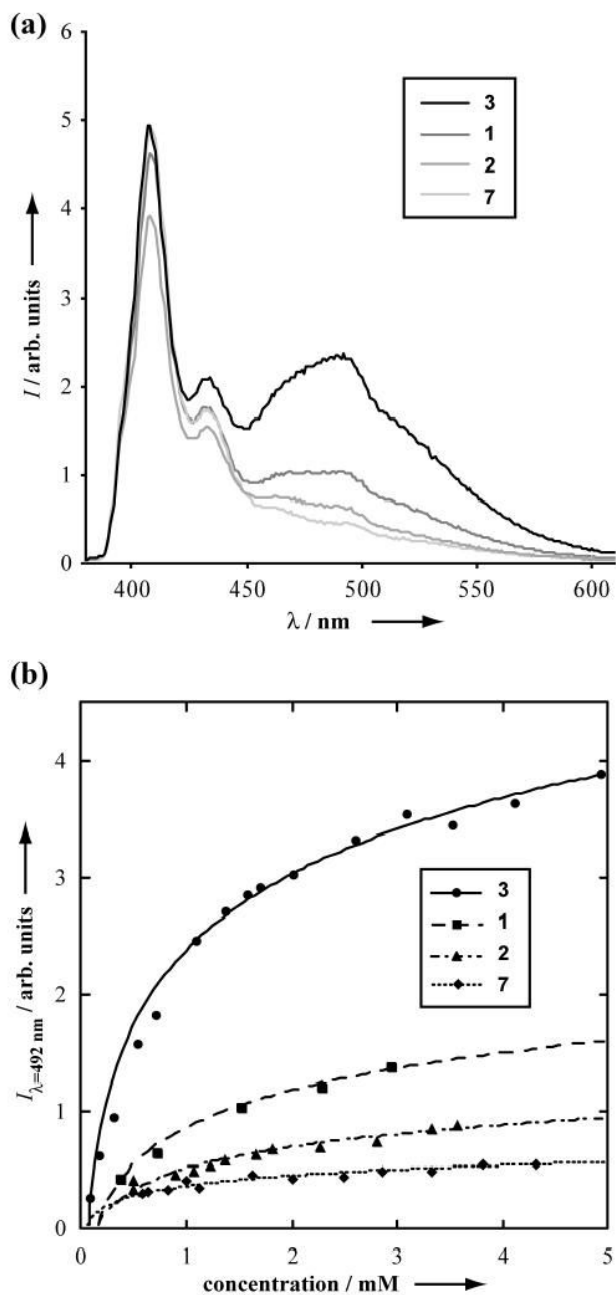
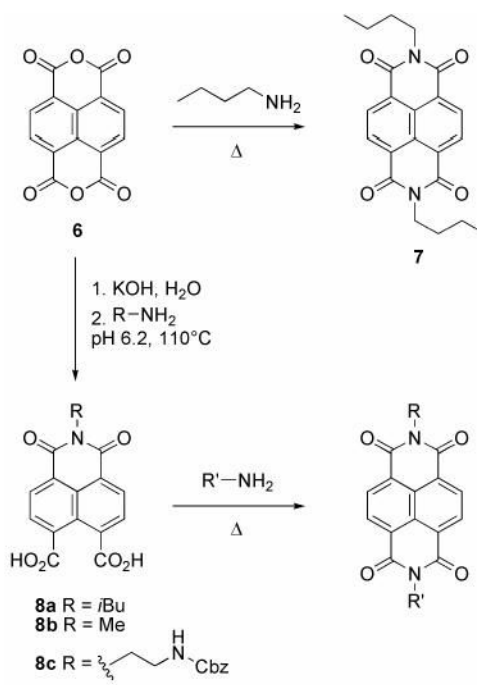
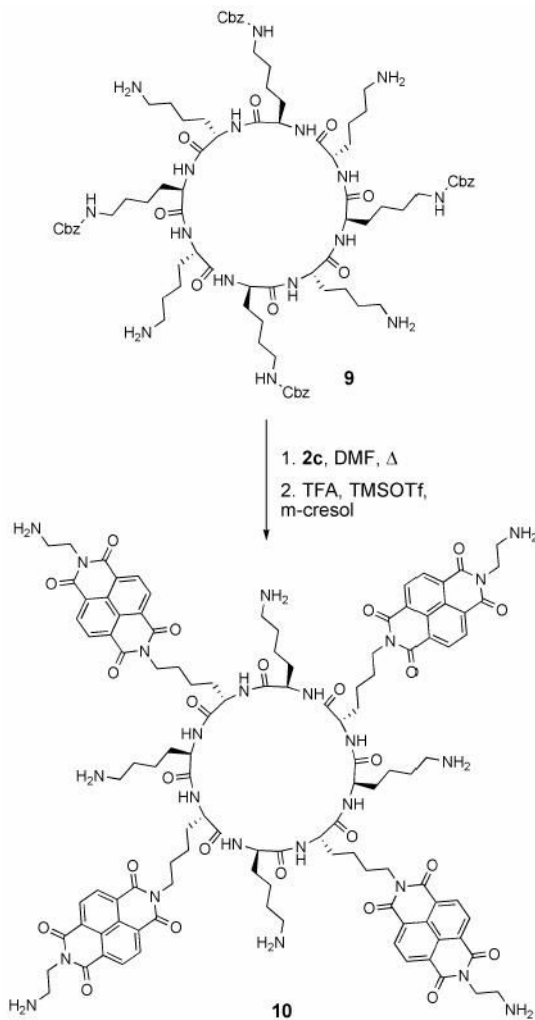


**Figure 3.**

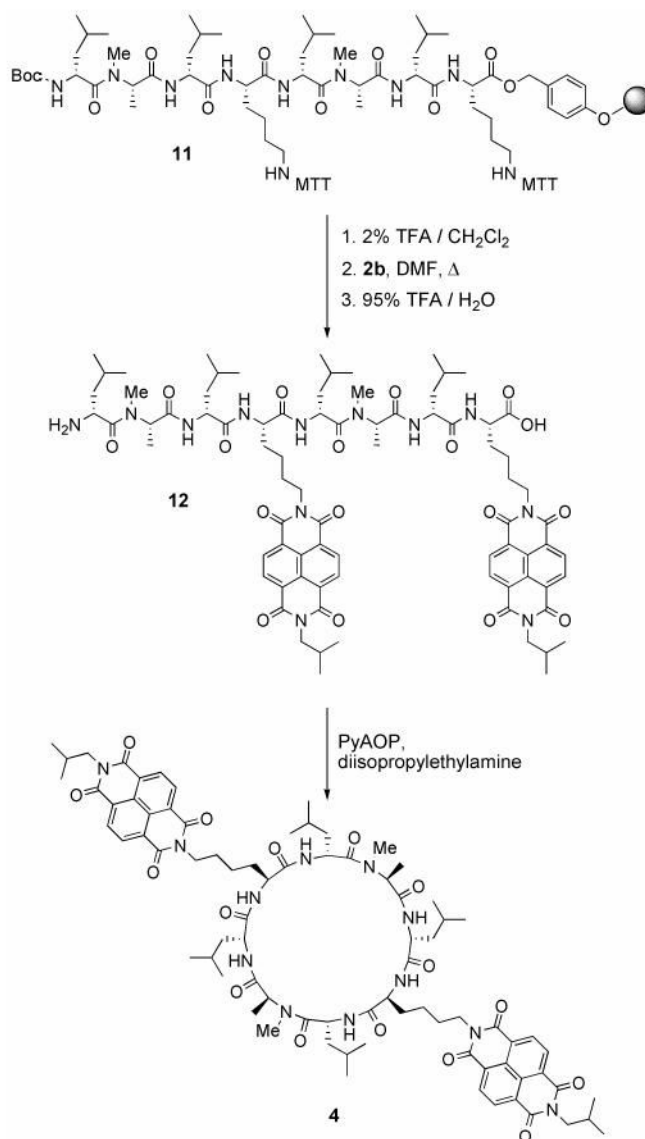
(a) Fluorescence spectra of 1.65 mM solutions of peptides **1**, **2**, **3**, and control compound **7** in  $\text{CDCl}_3$  ( $\lambda_{\text{ex}} = 330 \text{ nm}$ ); (b) the change in excimer intensity as a function of peptide concentration (lines are shown to guide the eye).



Scheme 1.



Scheme 2.



Scheme 3.

**Table 1**

Association constants as determined by NMR.

compound	Sequence <sup>[a]</sup>	$K_d$ <sup>[b]</sup> (M <sup>-1</sup> )
1	<i>cyclo</i> [Ala-Leu- <u>Me</u> Ala-Leu-Lys <sub>NDI-<i>i</i>Bu</sub> -Leu- <u>Me</u> Ala-Leu]	116
2	<i>cyclo</i> [Ala-Leu- <u>Me</u> Ala-Leu-Orn <sub>NDI-<i>i</i>Bu</sub> -Leu- <u>Me</u> Ala-Leu]	192
3	<i>cyclo</i> [Ala-Leu- <u>Me</u> Ala-Leu-Lys <sub>NDI-Me</sub> -Leu- <u>Me</u> Ala-Leu]	119
4	<i>cyclo</i> [(Lys <sub>NDI-<i>i</i>Bu</sub> -Leu- <u>Me</u> Ala-Leu) <sub>2</sub> ]	52
5	<i>cyclo</i> [(Orn <sub>NDI-<i>i</i>Bu</sub> -Leu- <u>Me</u> Ala-Leu) <sub>2</sub> ]	87
7	-	0.4

<sup>[a]</sup> underlined residues indicate D-enantiomers; MeAla = *N*-methyl-alanine;

<sup>[b]</sup> details of the calculations are found in the experimental.